Inorganic Chemistry
Article

Inorg. Chem. **2010**, *49*, 11287–11296 **11287**
DOI: 10.1021/ic1007389

Kinetics and Mechanism of Peroxymonocarbonate Formation

Ekaterina V. Bakhmutova-Albert, Huirong Yao, Daniel E. Denevan, and David E. Richardson*

Center for Catalysis, Department of Chemistry, University of Florida, Gainesville, Florida 32611-7200, United States

Received April 16, 2010

The kinetics and mechanism of peroxymonocarbonate (HCO_4^-) formation in the reaction of hydrogen peroxide with bicarbonate have been investigated for the pH 6−9 range. A double pH jump method was used in which ^{13}C-labeled bicarbonate solutions are first acidified to produce $^{13}CO_2$ and then brought to higher pH values by addition of base in the presence of hydrogen peroxide. The time evolution of the ^{13}C NMR spectrum was used to establish the competitive formation and subsequent equilibration of bicarbonate and peroxymonocarbonate following the second pH jump. Kinetic simulations are consistent with a mechanism for the bicarbonate reaction with peroxide in which the initial formation of CO_2 via dehydration of bicarbonate is followed by reaction of CO_2 with H_2O_2 (perhydration) and its conjugate base HOO^- (base-catalyzed perhydration). The rate of peroxymonocarbonate formation from bicarbonate increases with decreasing pH because of the increased availability of CO_2 as an intermediate. The selectivity for formation of HCO_4^- relative to the hydration product HCO_3^- increases with increasing pH as a consequence of the HOO^- pathway and the slower overall equilibration rate, and this pH dependence allows estimation of rate constants for the reaction of CO_2 with H_2O_2 and HOO^- at 25 °C (2×10^{-2} M^{-1} s^{-1} and 280 M^{-1} s^{-1}, respectively). The contributions of the HOO^- and H_2O_2 pathways are comparable at pH 8. In contrast to the perhydration of many other common inorganic and organic acids, the facile nature of the CO_2/HCO_3^- equilibrium and relatively high equilibrium availability of the acid anhydride (CO_2) at neutral pH allows for rapid formation of the peroxymonocarbonate ion without strong acid catalysis. Formation of peroxymonocarbonate by the reaction of HCO_3^- with H_2O_2 is significantly accelerated by carbonic anhydrase and the model complex $[Zn(II)L(H_2O)]^{2+}$ (L = 1,4,7,10-tetraazacyclododecane).

Introduction

There is considerable current interest in the interaction between hydrogen peroxide and carbon dioxide/carbonates in aqueous solution, particularly because of the potential biochemical importance of the chemistry.[1−13] In previous studies, we have explored the chemistry and reactivity of the peroxymonocarbonate ion (HCO_4^-), which is the covalent adduct of hydroperoxide ion (OOH^-) and CO_2.[10,14−17] It has been shown that the formation of this ion accounts for the observation that bicarbonate is an effective activator of hydrogen peroxide in the oxidation of nucleophiles, as initially proposed by Drago and co-workers.[18,19] Peroxymonocarbonate ion (or its kinetic equivalent) produced by the equilibrium reaction of bicarbonate with aqueous hydrogen peroxide (eq 1) is known to be the active oxidant in N- and

*To whom correspondence should be addressed. Phone: (352) 392-6736. E-mail: der@chem.ufl.edu.

(1) Augusto, O.; Bonini, M. *Free Radical Biol. Med.* **2004**, *36*, S20–S20.
(2) Bonini, M. G.; Gabel, S. A.; Ranguelova, K.; Stadler, K.; DeRose, E. F.; London, R. E.; Mason, R. P. *J. Biol. Chem.* **2009**, *284*, 14618–14627.
(3) Bonini, M. G.; Miyamoto, S.; Di Mascio, P.; Augusto, O. *J. Biol. Chem.* **2004**, *279*, 51836–51843.
(4) Cerchiaro, G.; Trindade, D. F.; Augusto, O. *Free Radical Biol. Med.* **2006**, *41*, S120–S120.
(5) Medinas, D. B.; Cerchiaro, G.; Trindade, D. F.; Augusto, O. *IUBMB Life* **2007**, *59*, 255–262.
(6) Medinas, D. B.; Toledo, J. C.; Cerchiaro, G.; Do-Amaral, A. T.; De-Rezende, L.; Malvezzi, A.; Augusto, O. *Chem. Res. Toxicol.* **2009**, *22*, 639–648.
(7) Medinas, D. B.; Toledo, J. C.; Cerchiaro, G.; Do-Amarat, A. T.; Rezende, L.; Malvezzi, A.; Augusto, O. *Free Radical Biol. Med.* **2008**, *45*, S20–S20.
(8) Ramirez, D. C.; Gomez-Mejiba, S. E.; Corbett, J. T.; Deterding, L. J.; Tomer, K. B.; Mason, R. P. *Biochem. J.* **2009**, *417*, 341–353.
(9) Richardson, D. E.; Regino, C. A. S.; Yao, H. R.; Johnson, J. V. *Free Radical Biol. Med.* **2003**, *35*, 1538–1550.
(10) Regino, C. A. S.; Richardson, D. E. *Inorg. Chim. Acta* **2007**, *360*, 3971–3977.
(11) Trindade, D. F.; Bonini, M.; Cunha, R.; Augusto, O. *Free Radical Biol. Med.* **2004**, *36*, S65–S65.
(12) Trindade, D. F.; Cerchiaro, G.; Augusto, O. *Chem. Res. Toxicol.* **2006**, *19*, 1475–1482.
(13) Yermilov, V.; Yoshie, Y.; Rubio, J.; Ohshima, H. *FEBS Lett.* **1996**, *399*, 67–70.
(14) Richardson, D. E.; Yao, H. R.; Frank, K. M.; Bennett, D. A. *J. Am. Chem. Soc.* **2000**, *122*, 1729–1739.
(15) Bennett, D. A.; Yao, H.; Richardson, D. E. *Inorg. Chem.* **2001**, *40*, 2996–3001.
(16) Yao, H. R.; Richardson, D. E. *J. Am. Chem. Soc.* **2003**, *125*, 6211–6221.
(17) Balagam, B.; Richardson, D. E. *Inorg. Chem.* **2008**, *47*, 1173–1178.
(18) Drago, R. S.; Frank, K. M.; Yang, Y.-C.; Wagner, G. W. *Activation of Hydrogen Peroxide*; U. S. Army Edgewood Research, Development and Engineering Center: Aberdeen Proving Ground, MD, 1998.
(19) Richardson, D. E.; Yao, H.; Xu, C.; Drago, R. S.; Frank, K. M.; Wagner, G. W.; Yang, Y.-C. *Kinetics and Equilibrium Formation of a Weakly Basic Oxidant System for Decontamination*; U. S. Army Edgewood Chemical Biological Center: Aberdeen Proving. Ground, MD, 1999.

Published on Web 11/15/2010

S- oxidation of tertiary amines,[17] organic sulfides,[14,15] and thiols.[10]

$$HCO_3^- + H_2O_2 = HCO_4^- \quad (1)$$

The peroxymonocarbonate ion has been isolated in various salts and characterized by Raman spectroscopy,[20,21] NMR,[14,20] and X-ray crystallography.[22] Theoretical studies of the oxidant and its chemistry have been reported recently.[23−28]

The anionic peracid HCO_4^- forms in water as well as in mixed organic-water solvents at near neutral pH values.[14,20] The equilibration of dilute bicarbonate solution with 1 M hydrogen peroxide has a half-life of ~10 min at 25 °C and pH 7.4.[29] The structure of peroxymonocarbonate, $HOOCO_2^-$,[22] is analogous to peroxides such as peroxymonosulfate ($HOOSO_3^-$), peroxynitrate (O_2NOO^-), and peroxyacetic acid ($CH_3C(O)OOH$). In contrast to HCO_4^-, those peroxo species can only be prepared practically by the reaction of their corresponding acids with hydrogen peroxide in strongly acidic aqueous solutions.[30−32] Strong acids are commonly used not only to catalyze the reaction but also to provide dehydrating conditions that favor equilibrium formation of peroxyacids.[33] Borate, like bicarbonate, is an exception and readily forms reactive peroxides in neutral to mildly alkaline solutions.[34] One goal of the present study was to provide a detailed mechanism that explains the facile formation of HCO_4^- from HCO_3^- via eq 1 in near neutral pH conditions.

In general, there is strong evidence that the conversion of peroxide to HCO_4^- provides a pathway for activation of peroxide for two-electron chemistry and radical chemistry, the latter in combination with transition metals. Kinetic evidence has been reported for the potential role of peroxymonocarbonate as a reactive oxygen species (ROS) in biology, particularly in the oxidation of sulfur-containing biomolecules.[9,10] The kinetic parameters for HCO_4^- oxidation of free methionine,[9] methionine in α1-proteinase inhibitor,[9] cysteine[10] and other thiols have been determined. It has been shown that the oxidation of methionine is accelerated by a carbonic anhydrase model complex (presumably by increasing the rate of HCO_4^- formation from bicarbonate).[9] Reports on the potential biological significance of related $Mn/H_2O_2/HCO_3^-$ chemistry[35−38] and the peroxidase reactivity of copper SOD in the presence of peroxide and bicarbonate[2,39−41] have also suggested a central role for the HCO_4^- ion. Peroxymonocarbonate has also been implicated in the chemistry of the manganese-catalyzed oxidation of C−C double bonds[42−44] and dyes[45,46] by mixtures of hydrogen peroxide and bicarbonate.

There have been only a few studies that mention the effect of hydrogen peroxide on the hydration rate for carbon dioxide. Kiese and Hastings[47] and Danckwerts and Sharma[48] reported that hydrogen peroxide is a weak catalyst for the hydration reaction, but their experimental methods would not distinguish catalysis of hydration from covalent adduct formation, since both pathways consume carbon dioxide.

We proposed[14] that the mechanism of formation of peroxymonocarbonate is analogous to the formation of bicarbonate from carbon dioxide in water. In the present work, we have investigated the kinetics of the formation of HCO_4^- at pH values in the range 6−9 in aqueous solution. The kinetic results from double pH jump experiments are consistent with a mechanism in which CO_2 is the key intermediate in this reaction. The rate constants for the reactions in the CO_2 perhydration/hydration equilibrium have been estimated from numerical simulations of ^{13}C NMR experimental results. We have also shown that the formation of HCO_4^- is accelerated by the presence of carbonic anhydrase, indicating significant catalysis of HCO_4^- formation when the rate of dehydration of HCO_3^- to CO_2 is increased. Catalysis by the carbonic anhydrase model Zn(II)L (L = 1,4,7,10-tetraazacyclododecane)[49] has also been examined, and the results support the proposed mechanism for peroxymonocarbonate formation via CO_2.

Experimental Section

Materials. 99% ^{13}C enriched sodium bicarbonate and 99.9% D_2O (Cambridge Isotope Laboratories) were used as received. Tribasic sodium phosphate dodecahydrate (Fisher), dibasic phosphate (Sigma), glacial acetic acid (Fisher), acetonitrile (Fisher), zinc perchlorate hexahydrate (Johnson Matthey) and 1,4,7,10-tetraazacyclododecane ([12]aneN_4, cyclen), all reagent grade, were used without further purification. Hydrogen peroxide (Aldrich, 35%) was standardized iodometrically. Water was purified by a Barnstead Nanopure System (resistance $> 10^{17}$ ohms).

Equilibration Kinetics. ^{13}C NMR studies on peroxycarbonate formation by mixing H_2O_2 (2.0 M) and 99% ^{13}C enriched $NaHCO_3$ (0.10 M) were performed as described previously.[29] Normally, 10% D_2O was employed for NMR instrument locking. The pH

(20) Flanagan, J.; Jones, D. P.; Griffith, W. P.; Skapski, A. C.; West, A. P. *J. Chem. Soc., Chem. Commun.* **1986**, 20–21.
(21) Jones, D. P.; Griffith, W. P. *J. Chem. Soc., Dalton Trans.* **1980**, 2526–2532.
(22) Adam, A.; Mehta, M. *Angew. Chem., Int. Ed.* **1998**, *37*, 1387–1388.
(23) Maetzke, A.; Jensen, S. J. K.; Csizmadia, I. G. *Chem. Phys. Lett.* **2007**, *448*, 46–48.
(24) Aparicio, F.; Contreras, R.; Galvan, M.; Cedillo, A. *J. Phys. Chem. A* **2003**, *107*, 10098–10104.
(25) Kieninger, M.; Mendez, P. S.; Ventura, O. N. *Chem. Phys. Lett.* **2009**, *480*, 52–56.
(26) Mendez, P. S.; Eriksson, L. A.; Ventura, O. N. *THEOCHEM* **2009**, *913*, 131–138.
(27) Quinonero, D.; Musaev, D. G.; Morokuma, K. *THEOCHEM* **2009**, *903*, 115–122.
(28) Saenz-Mendez, P.; Eriksson, L. A.; Ventura, O. N. *THEOCHEM* **2009**, *913*, 131–138.
(29) Richardson, D. E.; Yao, H.; Frank, K. M.; Bennett, D. *J. Am. Chem. Soc.* **2000**, *122*, 1729–1739.
(30) Greenspan, F. P. *J. Am. Chem. Soc.* **1946**, *68*, 907.
(31) Ball, E. *J. Am. Chem. Soc.* **1956**, *78*, 1125.
(32) Keith, W. G.; Powell, R. E. *J. Chem. Soc., A* **1969**, 90.
(33) Swern, D. In *Organic Peroxides*; Wiley: New York, 1970; pp 313−516.
(34) Davies, D. M.; Deary, M. E.; Quill, K.; Smith, R. A. *Chem.—Eur. J.* **2005**, *11*, 3552–3558.
(35) Berlett, B. S.; Chock, P. B.; Yim, M. B.; Stadtman, E. R. *Proc. Natl. Acad. Sci. U.S.A.* **1990**, *87*, 389–393.
(36) Yim, M. B.; Berlett, B. S.; Chock, P. B.; Stadtman, E. R. *Proc. Natl. Acad. Sci. U.S.A.* **1990**, *87*, 394–398.
(37) Liochev, S. I.; Fridovich, I. *J. Inorg. Biochem.* **2006**, *100*, 694–696.
(38) Liochev, S. I.; Fridovich, I. *Proc. Natl. Acad. Sci. U.S.A.* **2004**, *101*, 743–744.
(39) Bonini, M. G.; Fernandes, D. C.; Augusto, O. *Biochemistry* **2004**, *43*, 344–351.
(40) Liochev, S. I.; Fridovich, I. *Free Radical Biol. Med.* **1999**, *27*, 1444–1447.
(41) Liochev, S. I.; Fridovich, I. *Arch. Biochem. Biophys.* **2004**, *421*, 255–259.
(42) Lane, B. S.; Burgess, K. *Chem. Rev.* **2003**, *103*, 2457–2473.
(43) Lane, B. S.; Burgess, K. *J. Am. Chem. Soc.* **2001**, *123*, 2933–2934.
(44) Lane, B. S.; Vogt, M.; DeRose, V. J.; Burgess, K. *J. Am. Chem. Soc.* **2002**, *124*, 11946–11954.
(45) Ember, E.; Gazzaz, H. A.; Rothbart, S.; Puchta, R.; van Eldik, R. *Appl. Catal., B* **2010**, *95*, 179–191.
(46) Ember, E.; Rothbart, S.; Puchta, R.; van Eldik, R. *New J. Chem.* **2009**, *33*, 34–49.
(47) Kiese, M.; Hastings, A. B. *J. Biol. Chem.* **1940**, *132*, 267–280.
(48) Danckwerts, P. V.; Sharma, M. M. *Trans.Faraday Soc.* **1963**, *59*, 386–395.
(49) Zhang, X.; Van Eldik, R. *Inorg. Chem.* **1995**, *34*, 5606–5614.

of the solution consisting of H_2O_2 (2.0 M) and $NaHCO_3$ (0.10 M) was 7.4 in the absence of phosphate buffers. Adjustment of the pH of the solutions was achieved by addition of tribasic phosphate buffer (pH > 8.0) or acetic acid (pH < 7.0).

Kinetic Experiments on Peroxymonocarbonate Formation by Double pH Jump. ^{13}C NMR spectra were collected with a Mercury 300BB spectrometer at 0 °C. The temperature was calibrated with a standard methanol sample before each experiment. Acetonitrile was used as an internal chemical shift reference, and 20% D_2O was employed for instrument locking. The spectrometer was set to absolute intensity conditions. To retain the quantitative information in ^{13}C spectra, the relaxation delay and the acquisition times were 5 and 4 s, respectively, with 8 or 16 transients collected per spectrum to achieve acceptable signal-to-noise values. Peak intensities of NMR signals were analyzed by using the *kini* program in the Varian VNMR software.

All samples were prepared by mixing 99% ^{13}C enriched $NaHCO_3$ (0.1M) with glacial CH_3COOH (final concentration ~0.13 M) for complete conversion of bicarbonate into CO_2 followed by addition of H_2O_2 (to final concentration 1.0 M). Gas is released upon acidification. The final solutions were transferred into a 5 mm NMR tube with cap and septa and cooled down to 0 °C in an ice bath. A stock solution of sodium phosphate (0.5 M) was injected directly in the tube for pH adjustment (pH = 6−8). The sample was placed in a cold probe immediately, and the ^{13}C NMR spectra were recorded for 2−3 h, with the first spectrum typically acquired at $t \approx 400$ s following the second pH jump. The sample solution pH was measured at 0 °C after completion of the reaction.

Determination of Kinetic Product Distribution. Additional double pH jump experiments were done to determine the relative amounts of HCO_4^- and HCO_3^- produced at $t = 20$ s. These studies were performed on a Gemini 300 MHz NMR with the same delay and acquisition times described above. An appropriate volume of CH_3COOH was added initially in a mixture of H_2O_2 (2.0 M) and ^{13}C enriched $NaHCO_3$ (0.1 M) in an NMR tube. Bicarbonate was fully converted to CO_2, as indicated by disappearance of the HCO_3^- signal and formation of CO_2 ($\delta \approx$ 124.5 ppm) in the ^{13}C NMR spectrum. A stock solution of Na_3PO_4 (2 M) was added rapidly to the above solutions to adjust the pH to the desired value (pH = 6.7, 7.4, 8.0, and 8.5) at room temperature. The headspace of the NMR tube was quickly flushed with N_2 gas to reduce the amount of CO_2 gas left in the upper part of the tube. The tube was then immersed (normally 20 s after the addition of phosphate) in a liquid-N_2 bath to freeze the solution and stop further reaction. Upon insertion in a warm probe, a ^{13}C NMR spectrum of the sample solution was taken immediately when the sample reached 0 °C (when the solution thawed), and this spectrum was taken as the $t = 20$ s spectrum for the room temperature reaction. The final equilibrium ^{13}C NMR spectrum was recorded after 1−2 h at 25 °C after the sample warmed to the set temperature. The pH of the solution was measured at room temperature before and after the equilibrium reaction was completed.

Kinetic Experiments on Peroxymonocarbonate Formation in the Presence of Carbonic Anhydrase and Zinc Model Complex. A stock solution of 1,4,7,10-tetraazacyclododecanezinc(II), [[12]-aneN$_4$Zn(II)−OH$_2$](ClO$_4$)$_2$, was prepared in situ by dissolving 1:1 equiv of [12]aneN$_4$ and Zn(ClO$_4$)$_2$·6H$_2$O in water. The mixture was stirred for ~2 h before use. The ^{13}C NMR spectra were recorded on a Gemini 300 MHz spectrometer at 25 °C. 10% D_2O was used for instrument locking. Freshly prepared Zn(II) complex (final concentration 0.001−0.01M) was mixed with H_2O_2 (2 M) and 99% ^{13}C enriched $NaHCO_3$ (0.1M) directly in NMR tube before each measurement. The rate of equilibration was followed by the increasing intensities of the signal due to peroxymonocarbonate.

For ^{13}C NMR studies in the presence of carbonic anhydrase, ethanol−water (1:1 v:v) solvent was used. Typically, a solution of carbonic anhydrase (400 μg) in ethanol was mixed with H_2O_2 (2 M), an aqueous solution of 99% ^{13}C enriched bicarbonate (0.1 M), and the mixture was injected in an NMR tube immediately for measurements.

Scheme 1

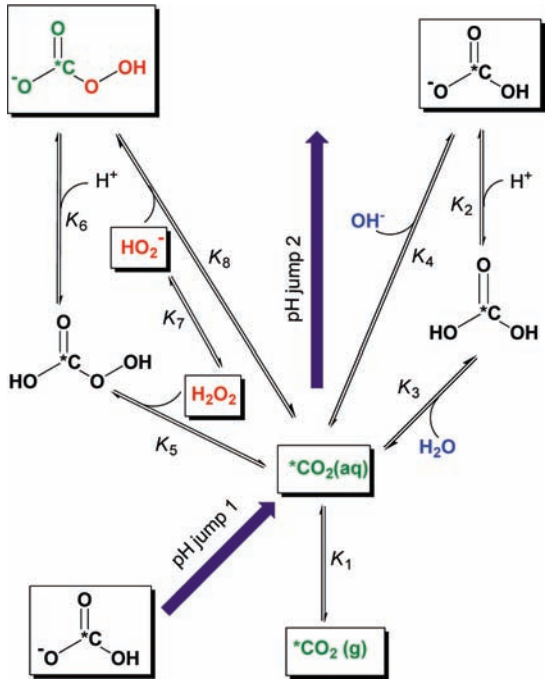

Kinetic Simulations. Kinetic simulations for CO_2 decay and formation of peroxymonocarbonate (HCO_4^-) were produced by using programs that perform numerical integrations for multistep mechanisms via the Gear method. These programs were written by L. Yao and D. E. Richardson, and the integrator is based on the Accuchem kinetics program.[50]

Results and Discussion

Equilibration Kinetics. On the basis of our previous work and by analogy to hydration-dehydration reactions for carbon dioxide/bicarbonate, we hypothesized that the mechanism of peroxymonocarbonate formation in eq 1 involves the intermediate formation of carbon dioxide followed by addition of peroxide. We have previously reported the kinetics and equilibration of peroxymonocarbonate formation followed by ^{13}C NMR in water or mixed aqueous solvents,[14] and the equilibrium constant K_{eq} for eq 1 has been determined again for the present work. The equilibrium constant $K_{eq} = 0.33 \pm 0.02\ M^{-1}$ at 25 °C (ref 14 reported $0.32 \pm 0.02\ M^{-1}$), and the $t_{1/2}$ for the reaction is ~5 min with $[H_2O_2] = 2.0$ M in unbuffered dilute bicarbonate solution. Similar studies of the equilibrium reaction were performed at pH values of 6.7 and 8.5 in water. The rate of equilibration decreases with increasing pH of the solution (at pH = 8.5, $t_{1/2} \approx 14$ min; at pH = 6.7, $t_{1/2} < 1$ min with $[H_2O_2] = 2.0$ M). These observations immediately suggest the involvement of carbon dioxide as the hydration-dehydration reaction rate for CO_2/HCO_3^- increases as the pH is lowered because of acid catalysis.[51]

(50) Braun, W.; Kahaner, D.; Herron, J. T. *Int. J. Chem. Kinet.* **1988**, *20*, 51–62.
(51) Palmer, D. A.; Van Eldik, R. *Chem. Rev.* **1983**, *83*, 651–731.

Table 1. Elementary Reactions and Their Equilibrium and Rate Constants for Simulation of Peroxymonocarbonate Formation (T = 0 °C and 25 °C)

		T = 0 °C		T = 25 °C	
	reaction	equilibrium constants[a]	rate constants[b]	equilibrium constants[c]	rate constants[c,d]
M1	$CO_2(g) = CO_2(aq)$		$k_1 = 2.0 \times 10^{-3}\ s^{-1}$		
M2	$HCO_3^- + H^+ = H_2CO_3$	$K_2 = 2.33 \times 10^3\ M^{-1}$	$k_2 = 1.40 \times 10^{11}\ M^{-1}\ s^{-1}$ $k_{-2} = 6.01 \times 10^7\ s^{-1}$	$K_2 = 3.5 \times 10^3\ M^{-1}$	$k_2 = 1.4 \times 10^{11}\ M^{-1}\ s^{-1}$ $k_{-2} = 4.0 \times 10^7\ s^{-1}$
M3	$H_2CO_3 = CO_2(aq)$	$K_3 = 8.01 \times 10^2$	$k_3 = 3.74\ s^{-1}$ $k_{-3} = 4.67 \times 10^{-3}\ s^{-1}$	$K_3 = 3.87 \times 10^2$	$k_3 = 1.16 \times 10^1\ s^{-1}$ $k_{-3} = 3.0 \times 10^{-2}\ s^{-1}$
M4	$HCO_3^- = CO_2(aq) + HO^-$	$K_4 = 2.00 \times 10^{-9}$ M	$k_4 = 4.42 \times 10^{-6}\ s^{-1}$ $k_{-4} = 2.07 \times 10^3\ M^{-1}\ s^{-1}$	$K_4 = 2.34 \times 10^{-8}$ M	$k_4 = 1.99 \times 10^{-4}\ s^{-1}$ $k_{-4} = 8.5 \times 10^3\ M^{-1}\ s^{-1}$
M5	$CO_2(aq) + H_2O_2 = H_2CO_4$	$K_5 = 4.12 \times 10^{-4}\ M^{-1}$	$k_5 \geq 1.6 \times 10^{-2}\ M^{-1}\ s^{-1}$ $k_{-5} \geq 3.76 \times 10^1\ s^{-1}$	$K_5 = 8.5 \times 10^{-4}\ M^{-1}$	$k_5 = 1.9 \times 10^{-2}\ M^{-1}\ s^{-1}$ $k_{-5} = 2.2 \times 10^1\ s^{-1}$
M6	$H_2CO_4 = HCO_4^- + H^+$	$K_6 = 4.29 \times 10^{-4}$ M	$k_6 = 6.01 \times 10^7\ s^{-1}$ $k_{-6} = 1.40 \times 10^{11}\ M^{-1}\ s^{-1}$	$K_6 = 2.86 \times 10^{-4}$ M	$k_6 = 4.0 \times 10^7\ s^{-1}$ $k_{-6} = 1.4 \times 10^{11}\ M^{-1}\ s^{-1}$
M7	$H_2O_2 = HOO^- + H^+$	$K_7 = 7.01 \times 10^{-13}$ M	$k_7 = 9.81 \times 10^{-2}\ s^{-1}$ $k_{-7} = 1.40 \times 10^{11}\ M^{-1}\ s^{-1}$	$K_7 = 1.58 \times 10^{-12}$ M	$k_7 = 0.22\ s^{-1}$ $k_{-7} = 1.4 \times 10^{11}\ M^{-1}\ s^{-1}$
M8	$CO_2(aq) + HOO^- = HCO_4^-$	$K_8 = 2.52 \times 10^5\ M^{-1}$	$k_8 \geq 1.1 \times 10^3\ M^{-1}\ s^{-1}$ $k_{-8} \geq 4.29 \times 10^{-3}\ s^{-1}$	$K_8 = 1.13 \times 10^5\ M^{-1}$	$k_8 = 2.8 \times 10^2\ M^{-1}\ s^{-1}$ $k_{-8} = 1.8 \times 10^{-3}\ s^{-1}$
M9[e]	$HCO_3^- + ZnL(H_2O)^{2+} = CO_2 + ZnL(OH)^+$			$K_9 = 1.7 \times 10^{-2}$	$k^d_{cat} = 56\ M^{-1}\ s^{-1}$ $k^h_{cat} = 3.3 \times 10^3\ M^{-1}\ s^{-1}$

[a] See text for sources of equilibrium constant values. The value of K_6 was estimated as $1/K_2$. The values for K_5 and K_8 were determined from eqs 2 and 3. [b] See text for sources of rate constants estimated from literature sources. Values for reactions M5 and M8 were estimated in this work. [c] The rate constants and equilibrium constants used in simulations are from ref 56 and references therein, unless otherwise specified. The value of K_6 was estimated as $1/K_2$. The values for K_5 and K_8 were determined from eqs 2 and 3. [d] Rate constants for reactions M5 and M8 are from the best fit to experimental data in this work. [e] Rate constants were taken from reference 49. Reaction M9 is only included in simulations for experiments where the catalyst $[Zn(II)L(H_2O)]^{2+}$ (L = 1,4,7,10-tetraazacyclododecane) was used.

The general mechanism used in this work for the simulations and data fitting is shown in Scheme 1, where the relevant equilibrium constants are shown. The right side of Scheme 1 shows the well-known hydration-dehydration reactions of CO_2 in water, and the left side shows the analogous perhydration-deperhydration reactions. In one perhydration pathway, the addition of H_2O_2 to form percarbonic acid is followed by deprotonation to form the HCO_4^- ion observed in neutral and weakly alkaline solutions. In the second pathway, the direct addition of OOH^- to CO_2 forms HCO_4^- in its thermodynamically stable protonation state as determined by structural methods.[22] In addition, each equilibrium is accompanied by forward and reverse rate constants, indicated by k_n and k_{-n}, where n is the label for the corresponding equilibrium constant K_n. All mechanistic steps (labeled Mn) used in simulations and data fitting described below are listed in Table 1.

The literature values for equilibrium and rate constants in Table 1 were obtained for 0 °C from published temperature dependences,[51−55] except for reactions M5, M6, and M8. The value of K_2 (reaction M2) was calculated from the equilibrium constant for CO_2 acid dissociation.[53] Rate constants for the CO_2 hydration equilibrium (reaction M3)[52] were used to calculate K_3. The rate constant for the $HCO_3^- \rightarrow CO_2 + OH^-$ reaction and the equilibrium constant (K_7) for hydrogen peroxide deprotonation are known,[54,55] and K_w is 1.15×10^{-15} at 0 °C. To account for the buffered pH value, reactions involving the proton were simulated by using the calculated pseudo first-order rate constant from $k = k_n\,[H^+]$, where $[H^+]$ is obtained from the buffer pH value.

K_5 and K_8 were calculated based on eqs 2 and 3. The equilibrium constant for eq 1 was found to have negligible temperature dependence between 0 and 25 °C, and a value of $K_{eq} = 0.33$ was used throughout this work. It was usually assumed $pK_a\,(H_2CO_4) = pK_a\,(H_2CO_3) = 3.4$ to estimate K_6 in eq 2 (other assumptions about this value were also considered; see discussion below).

$$K_{eq} = K_2K_3K_5K_6 \quad (2)$$

$$K_{eq} = K_2K_3K_7K_8 \quad (3)$$

An alternate set of constants from the work of Pyror et al.[56] for room temperature were used to simulate experiments designed to capture the kinetic product distribution of HCO_4^- and HCO_3^-. The rate constants and equilibrium constants used in room temperature simulations are listed in Table 1. A literature value of $pK_a\,(H_2O_2) = 11.8$ is used in the room temperature simulations.[55] The initial concentration of CO_2 used in room temperature simulations was set to be its saturating concentration (0.03 M) in water, though a higher (0.05 M) or lower (0.02 M) initial concentration of CO_2 does not change the simulation results for rate constants. The complete profiles for concentrations of CO_2, HCO_3^-, and HCO_4^- versus reaction time were obtained by simulations of kinetic mechanisms at various pH values.

Previous Kinetic Studies on the Reaction of Hydrogen Peroxide with CO_2. In this section we will review the literature in light of the spectroscopic evidence that the reaction of hydrogen peroxide and carbon dioxide produces the peroxymonocarbonate ion and its conjugate base (CO_4^{2-}) at neutral to alkaline pH values. In earlier work described in the literature,[47,48,57] the effect of peroxide was believed to reflect catalysis of the CO_2 hydration reaction rather than stable adduct formation. It is clear from the direct spectroscopic evidence in our work and that of others that

(52) Soli, A. L.; Byrne, R. H. *Mar. Chem.* **2002**, *78*, 65–73.
(53) Harned, H. S.; Bonner, F. T. *J. Am. Chem. Soc.* **1945**, *67*, 1026–1031.
(54) Welch, M. J.; Lifton, J. F.; Seck, J. A. *J. Phys. Chem.* **1969**, *73*, 3351–3356.
(55) Evans, M. G.; Uri, N. *Trans. Faraday Soc.* **1949**, *45*, 224–230.
(56) Pryor, W. A.; Lemercier, J. N.; Zhang, H.; Uppu, R. M.; Squadrito, G. L. *Free Radical Biol. Med.* **1997**, *23*, 331–338.
(57) Dennard, A. E.; Williams, R. J. P. *J. Chem. Soc., A* **1966**, 812–816.

the disappearance of CO_2 in the presence of hydrogen peroxide is accelerated primarily by stable adduct formation rather than acid−base catalysis or transient adduct formation. Catalytic mechanisms for hydration do not assume the buildup of significant concentrations of intermediate adducts of catalyst with CO_2, but the usual measurement method (manometry of CO_2 absorption by an aqueous solution of buffers and catalyst) cannot distinguish between adduct formation and hydration, both of which remove CO_2 from the gas phase.

In 1939, Kiese and Hastings[47] noted that H_2O_2 at a concentration of 0.05 M doubled the rate of hydration at pH 6.9 and 5 °C, but they did not provide a further kinetic analysis. It is notable, however, that this "catalysis" was comparable to that by phosphate ion, which is regarded as a weak catalyst. In 1962, Danckwerts and Sharma[48] published a thorough study of the catalysis of hydration by many Brønsted bases at 0 °C, including H_2O_2. They analyzed the data by using the rate equation $R = \{k_u + k([B^-] + [HB])\}[CO_2]$, where k_u is the uncatalyzed rate constant, $[B^-] + [HB]$ represents the total concentration of the base and its conjugate acid, and k is the observed catalytic rate constant. Unfortunately, the data for hydrogen peroxide are sparse in their work, with a catalytic rate constant k at pH 7.52 recorded as 0.03 M^{-1} s^{-1} in phosphate buffer (0.05 M H_2O_2; adjustments were made for the weak catalysis by the buffer). The observation is in accord with that of Kiese and Hastings,[47] since 0.05 M peroxide would roughly double the uncatalyzed rate. Compared to many other bases, H_2O_2/OOH^- is an extremely weak "hydration catalyst."

Using the Danckwerts and Sharma value for k we can estimate the value of k_B, which is the rate constant for the "catalysis" by OOH^-, assuming the basic form is solely responsible for the reaction (the usual case with, for example, buffer catalysis). Using pK_a (H_2O_2) = 12 for 0 °C we estimate $k_B \approx 10^3$ M^{-1} s^{-1}, and the overall rate is given by $R = (k_u + k_B[OOH^-])[CO_2]$. Alternatively, if only H_2O_2 were acting as the "catalyst" the rate expression would be $R = k_u + k[H_2O_2][CO_2]$, where k = 0.03 M^{-1} s^{-1}.

Dennard and Williams[57] further investigated CO_2 hydration catalysis and remarked on the observation that among α-nucleophiles studied hypohalites (OCl^- and OBr^-) are strong catalysts while OOH^- and oximates are not. Given the lack of correlation with pK_a values of the α-nucleophiles, the authors suggested that strongly catalytic ions serve both as good nucleophiles and good leaving groups, a property that is not well correlated with pK_a values.

Double pH Jump Experiments. Since indirect methods (such as following CO_2 consumption by manometry) cannot distinguish covalent adduct formation from catalysis of hydration, we decided to observe the progress of the CO_2 reactions via NMR using ^{13}C-labeled bicarbonate as the starting material. To follow the hydration and perhydration reactions of CO_2, double pH jump experiments were carried out at low temperature (0 °C), which was the experimental temperature for the work of Danckwerts and Sharma.[48]

First, 99% enriched CO_2 was generated from labeled bicarbonate in situ by addition of acetic acid, which was chosen because carboxylates are reported to be inactive as hydration catalysts.[57] The ^{13}C NMR spectrum of the resulting solution, mixed with H_2O_2 (1 M), has a CO_2 peak at ∼124.5 ppm, and neither H_2CO_3/HCO_3^- nor H_2CO_4/HCO_4^- signals were detected in the spectrum. These observations indicate the complete conversion of bicarbonate to CO_2 via reactions in eqs 4 and 5 (i.e., the forward reactions for M2 and M3, Table 1).

$$HCO_3^- + H^+ \rightarrow H_2CO_3 \quad (4)$$

$$H_2CO_3 \rightarrow CO_2(aq) \quad (5)$$

Since only CO_2 is observed in the presence of concentrated H_2O_2 (1−2 M), the equilibrium of

$$CO_2(aq) + H_2O_2 = H_2CO_4 \quad (6)$$

eq 6 is strongly favored to the left as for the analogous carbon dioxide hydration equilibrium.

A second pH jump was achieved by addition of tribasic sodium phosphate, which has a small but known catalytic activity in carbon dioxide hydration.[57] The overall double pH jump sequence is illustrated in Scheme 1. By varying the amount of phosphate added to the acidic solution, the final pH value could be set by the resulting phosphate buffer. Two new NMR signals at ∼158.9 and ∼160.4 ppm appear as a result of the pH jump and are attributed to the formation of HCO_4^- and HCO_3^-, respectively.[14,20]

At pH values of ∼8 and lower reactions M2 and M3 are responsible for most of the formation of bicarbonate, while at higher pH values reaction M4 contributes significantly. The formation of peroxymonocarbonate is proposed to arise from one or both of two pathways, that is, the perhydration of CO_2 followed by deprotonation (the forward reactions for M5 and M6 in Table 1, also shown as eqs 7 and 8) or the direct reaction of CO_2 with OOH^- (base-catalyzed perhydration, that is, reaction M8 in Table 1, also shown as eq 9).

$$CO_2(aq) + H_2O_2 \rightarrow H_2CO_4 \quad (7)$$

$$H_2CO_4 \rightarrow HCO_4^- + H^+ \quad (8)$$

$$CO_2(aq) + HOO^- \rightarrow HCO_4^- \quad (9)$$

NMR spectra (Figure 1) show that the relative amount of peroxymonocarbonate produced around t = 400 s (typically the first spectrum in the 0 °C experiments) depends on the pH value. At pH 6.8, roughly equal amounts of HCO_4^- and HCO_3^- are observed, while an increase in pH causes a significant increase in the HCO_4^-/HCO_3^- ratio (Figure 1). The origin of the increase in the ratio at higher pH values will be discussed below.

The relative amounts of HCO_4^- and HCO_3^- change with time from the initial product distribution at t = 400 s as the eq 1 equilibration occurs. Two examples are shown in Figure 2. The observed rate constant (k_{obs}, s^{-1}) for equilibration (eq 1) was calculated for various pH values based on the decay of HCO_4^- NMR signal up to ∼5000 s. The results show that the equilibration rate decreases with increasing pH of the solution (Figure 3). The k_{obs} values determined from double pH jump experiments are consistent with our previous results (k_{obs} = 1.96 × 10^{-3} s^{-1}, pH = 7.4 at 25 °C),[14] considering the temperature difference,

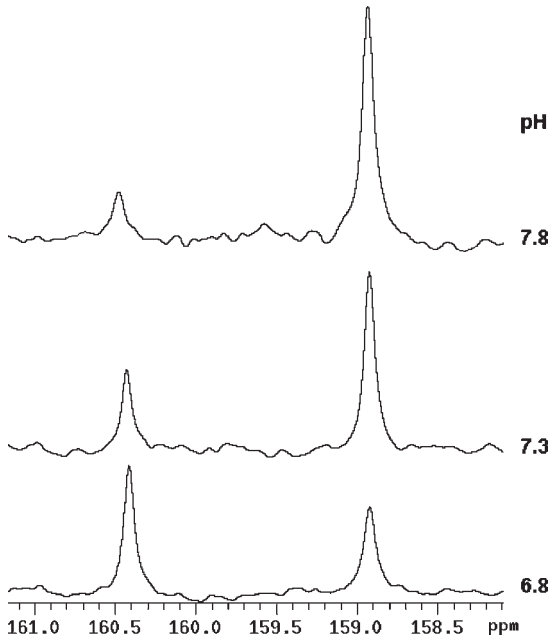

Figure 1. Selected ^{13}C NMR spectra of CO_2/H_2O_2 solutions recorded ~400 s after addition of base for the second pH jump ($T = 0$ °C, $[H_2O_2] = 1.0$ M). The peak at 158.9 ppm is assigned to the HCO_4^- ion and the peak at 160.4 ppm is assigned as HCO_3^-.

and are in a good agreement with the observed rate constant estimated by kinetic measurement of the direct reaction of HCO_3^- with 1 M H_2O_2 at higher pH values (e.g., $k_{obs} = 7.15 \times 10^{-5}$ s^{-1}, pH = 8.6). If the mechanism of Scheme 1 is correct, we should be able to simulate the kinetic behavior of all three carbon species during the entire course of the reaction in the double pH jump experiments.

Integration of the spectra at different t values showed that the total amount of carbon-13 in solution increases during the reaction because of $^{13}CO_2$(g) transfer from the head space of the NMR tube into the solution phase following the second pH jump. The transfer of gaseous $^{13}CO_2$, produced by the first pH jump, into the solution was introduced in the mechanism (reaction M1) with a rate constant k_1 that modeled the observed increase in the total ^{13}C intensity with time. The initial concentrations for [$^{13}CO_2$(g)] and [$^{13}CO_2$(aq)] were set to yield the best overall fit, and the transfer from the headspace generally accounted for a relatively small increase in total concentration as the reaction progressed (~10−20%). The dissolution of headspace $^{13}CO_2$ is effectively irreversible because of the subsequent reactions with water and peroxide at the high pH values after the second pH jump. Independent experiments on the transfer of CO_2 from the headspace into basic solutions showed that the relatively rapid transfer to solution (over a period of up to ~30 min) is not a consequence of enhanced mixing in a spinning NMR tube; the rate of transfer is comparable to that for a control tube that is not in the probe. Instead, CO_2 at the gas−liquid interface presumably reacts in the concentrated buffer in the diffusion layer, and the transfer of gas into solution appears to be more rapid than expected for simple diffusion as a result.

The hydration-dehydration rate constants (reaction M3) were changed somewhat to satisfy the best fit with experiment

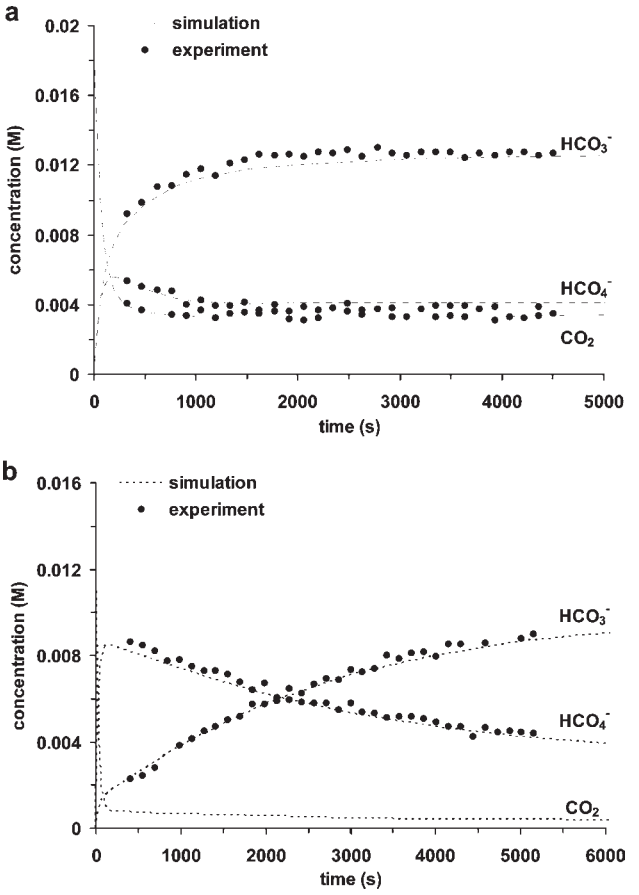

Figure 2. Examples of simulated and observed data (best fit) for CO_2 hydration and perhydration reactions at pH 6.8 (a) and 7.8 (b) ($T = 0$ °C, $[H_2O_2] = 1.0$ M), The mechanism used for the simulated curves includes reaction M8; reaction M5 is not included for the fits shown.

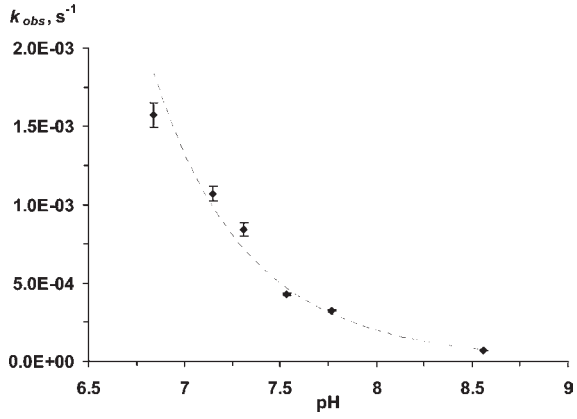

Figure 3. Observed rate constant of equilibration, k_{obs} (s^{-1}), as a function of pH ($T = 0$ °C, $[H_2O_2] = 1.0$ M).

and are consistent with the value for the rate constant determined by Danckwerts and Sharma[48] for phosphate-catalyzed hydration of CO_2. We assume that the small modifications in rate constants we made account for the weak phosphate catalysis in the double pH jump final solutions, and the values used (Table 1) are therefore somewhat higher than the uncatalyzed rate constants.[52] The mechanism also includes perhydration-deperhydration steps (M5, M8) with rate constants determined by the fits to the experimental data for values of k_5 and k_8. Values

for the corresponding reverse rate constants (k_{-5}, k_{-8}) were determined by the overall equilibrium constants as required by eqs 2 and 3.

There are two possible pathways for perhydration of CO_2 as shown in Scheme 1, and one or the other may dominate depending on their relative rate constants and the pH value. On the other hand, both pathways may contribute significantly in the experimental pH range. Deducing the relative contributions and rate constants can in principle be achieved by fitting of the kinetic model (reactions M1−M8) to the experimental results.

We first made the assumption that only OOH^- contributes to the formation of HCO_4^- (reactions M7 and M8, with reactions M5 and M6 omitted). On the basis of a fit to the observed time dependencies in the NMR data at multiple pH values, we find that $k_8 \geq 1100\ M^{-1}\ s^{-1}$. This value represents a minimum since larger values do not reduce the quality of the fit to the experimental data at $t = 400$ s and longer with a mean error exceeding 10%. The minimum value of 1100 $M^{-1}\ s^{-1}$ is consistent with the estimate derived above from the Danckwerts and Sharma[48] data assuming only base-catalyzed perhydration contributes.

Alternatively, reactions M5 and M6 can be used to produce the peroxymonocarbonate ion (i.e., reactions M7 and M8 are omitted). In this case, fits to the experimental kinetic data yield a best fit value of $k_5 \geq 0.016\ M^{-1}\ s^{-1}$. Again, increasing the rate constant above this minimum does not significantly decrease the accuracy of the fit for any of the pH values examined using a 10% allowable error. The minimum value is also close to that of 0.03 $M^{-1}\ s^{-1}$ quoted by Danckwerts and Sharma as the overall "catalysis" constant for H_2O_2. For the data we collected at 0 °C, starting at $t = 400$ s, reactions M1−M4 with either M5/M6 or M7/M8 are sufficient to fit the kinetic data over the pH range we studied, and the values of the derived rate constants are only minima. This ambiguity can be resolved by rapid quench double pH jump reactions as described in the next section.

The equilibrium constants K_5 and K_8 are determined based on the assumption that $pK_a(H_2CO_4)$ is 3.4 (reaction M6). We also examined simulation fits with $pK_a = 2.4$ and 4.4, respectively (the lower value may be the better estimate, since peroxy acids are more acidic than the related oxy acids,[58] for example, $pK_{a1}(H_3PO_5) = 1.1$ and $pK_{a1}(H_3PO_4) = 2.1$). The quality of the fits and the derived values of k_5 and k_8 are not affected.

Figure 2 shows an example of the best fit to observed data for all carbon species in solution at pH 6.8 and 7.8 using only the OOH^- mechanism (reactions M1−M4, M7, and M8). Rapid decay of CO_2 and formation of HCO_4^- and HCO_3^- occurs followed by slower equilibration to reach the thermodynamic equilibrium concentrations. Higher pH values increase the amount of peroxymonocarbonate produced relative to bicarbonate in the first 400 s (Figure 1). The difference in the relative concentrations as the pH is changed cannot be simply attributed to the acceleration of the CO_2 reaction with peroxide to form HCO_4^- in preference to HCO_3^-. The rate of equilibration is also pH dependent. The overall reaction of eq 1 equilibrates faster at lower pH values, and the equilibration reaction has proceeded significantly at $t = 400$ s at pH 6.7, thereby increasing the observed bicarbonate concentration at the expense of peroxymonocarbonate. At the higher pH value, equilibration via eq 1 has not proceeded to a significant extent at $t = 400$ s, and the initially observed peroxymonocarbonate concentration is determined primarily by the rate of the OOH^-/H_2O_2 addition to CO_2 compared to the hydration rate (Figure 2b).

An increase in k_5 or k_8 above the lower limits noted above affects only the first ~400 s of the reaction, where experimental data are not available on the time scale of NMR data collection in our low temperature experimental design. For example, considering only reaction M8 and raising k_8 by a factor of 5 increases the amount of HCO_4^- formation at its maximum in the simulation. However the model still fits the experimental data with at least 90% confidence (e.g., compare traces 2 and 3 in Figure 4a). Similar behavior is observed for k_5 changes with reaction M8 removed from the mechanism. In other words, the actual kinetic product distributions from competitive hydration and perhydration cannot be determined at a 400 s reaction time, and a shorter reaction time is required.

pH Jump Studies of HCO_4^- Formation with Rapid Quench. The simulations above suggested that we would need double pH jump experiments with very short reaction quench times (~20 s) to capture the true kinetic product distributions and identify the relative contributions of the two pathways (M5/M6 or M7/M8) to the overall reactions. These rapid quench reactions were done at 25 °C.

The pH dependence of the initial ratio $[HCO_4^-]/[HCO_3^-]$ ($t \approx 20$ s) determined by ^{13}C NMR spectroscopy in the pH jump experiments is shown in Figure 5. Once again, the rate of equilibration (eq 1) that followed was not different from that obtained directly by kinetic measurement of HCO_4^- formation via reaction of the HCO_3^- with H_2O_2 at room temperature.

The reactions used to model the experimental observations at room temperature are given in Table 1. Known rate constants at 25 °C are used for the hydration−dehydration reactions, and the mechanism includes perhydration-deperhydration reaction rate constants (reactions M5 and M8) determined by fitting the mechanism to the experimental data. Figure 6 shows the simulated decay of CO_2 and HCO_3^-/HCO_4^- equilibrium formation with $[CO_2]_0 = 0.03$ M and $[H_2O_2]_0 = 2.0$ M at pH = 8.5 at 25 °C. As in the low temperature experiments, at pH = 8.5 CO_2 decays rapidly to form HCO_3^-/HCO_4^- (no CO_2 is detected in the final spectrum), and the competition of perhydration and hydration initially yields more HCO_4^- than HCO_3^-. The similarity of the experimental observations for the HCO_3^-/HCO_4^- ratios at ~20 s and at ~400 s, especially at low pH values, suggests that the perhydration rate constants for either M5 and M8 are not significantly higher than the minimum estimates from the fitting described above (see, e.g., Figure 4a, where a much higher perhydration constant would predict a low HCO_3^-/HCO_4^- ratio at $t = 20$ s, but Figure 5 shows comparable amounts of HCO_3^- and HCO_4^- are formed).

Kinetic simulations of the rapid quench experiments at various pH values were used to find best-fit values for k_5 and k_8 with both reactions included in the simulation (0.019 $M^{-1}\ s^{-1}$ and 280 $M^{-1}\ s^{-1}$, respectively). Figure 7

(58) Battaglia, C. J.; Edwards, J. O. *Inorg. Chem.* **1965**, *4*, 552–558.

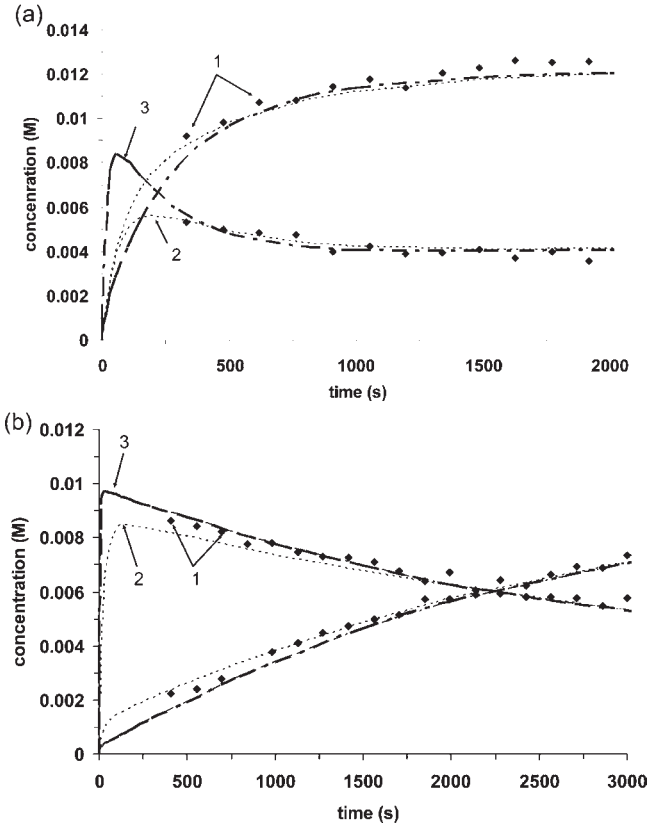

Figure 4. Effect of k_8 rate constant increase on the simulation of observed data at pH 6.8 (a) and 7.8 (b): 1, experiment (♦); 2, simulation with k_8 from the best fit; 3, simulation with k_8 increased by the factor of 5. The mechanism used here includes reaction M8 only; reaction M5 is not used for the fits. (T = 0 °C, [H_2O_2] = 1.0 M).

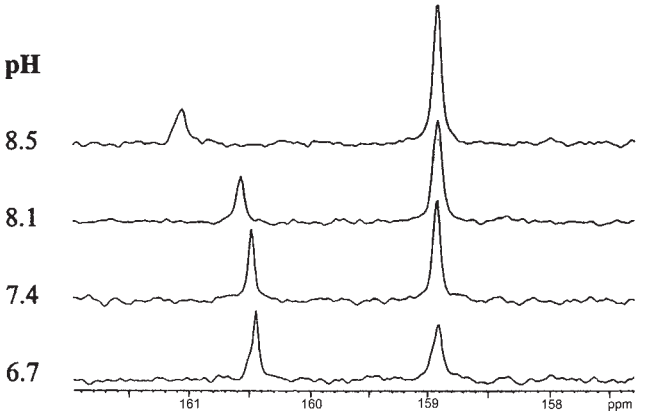

Figure 5. Representative ^{13}C NMR spectra of double pH jump solutions immediately after the addition of base to $^{13}CO_2$ solutions (t = 20 s, 25 °C, [H_2O_2] = 2.0 M). At higher pH values the amount of peroxymonocarbonate (at chemical shift ~159 ppm) produced relative to bicarbonate (~160−161 ppm) is enhanced because of the increase in the fraction of the CO_2 reactions with H_2O_2 and OOH^-. The shift in the bicarbonate signal toward higher chemical shifts is the result of increased formation of carbonate at higher pH values. The corresponding shift on the peroxymonocarbonate peak (because of equilibrium formation of CO_4^{2-}) occurs above pH 8 since the pK_a of HCO_4^- is somewhat higher than that of HCO_3^-.

shows that the model values of the initial ratio of $[HCO_4^-]/[HCO_3^-]$ (solid line) agree with the experimental data at $t \approx 20$ s. The other curves in Figure 7 show the impact on the fit of small variations of optimized parameters k_5 (and k_{-5}) and k_8 (and k_{-8}), illustrating how

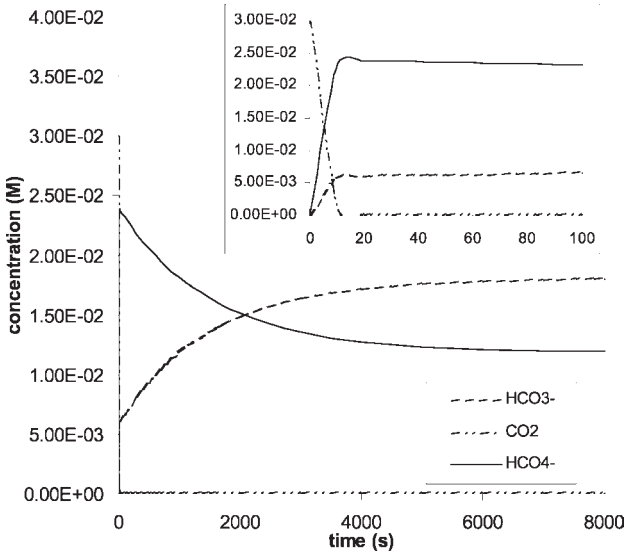

Figure 6. Simulation curves for CO_2 hydration and perhydration reactions. $[H_2O_2]_0$ = 2.0 M, $[CO_2]_0$ = 0.03 M, pH = 8.5. The perhydration of CO_2 is significantly more rapid than the hydration reaction under these conditions, leading to observed initial burst of peroxymonocarbonate formation followed by equilibration of eq 1. The inset shows the simulation of the first 100 s of the reaction. The experimental determination of the ratio $[HCO_4^-]/[HCO_3^-]$ was done at $t \approx 20-90$ s, and the observed ratios are unchanged over that range, as predicted by the simulation.

tightly the parameters are defined by the data. The primary determinants of the best fit values come from the higher pH experiments in which the kinetic products are most accurately determined since the equilibration that follows (eq 1) is much slower at the higher pH values. In addition, the values of $[HCO_4^-]/[HCO_3^-]$ under the experimental conditions do not vary significantly within a reaction time period of 10−60 s (i.e., during the NMR acquisition), and we conclude that the errors of rate constants k_5 and k_8 reported in Table 1 should not exceed ~30%, assuming the reactions for hydration and dehydration are accurately modeled.

Mechanism of CO_2 Reaction with Hydrogen Peroxide. From the kinetic analysis we conclude that the mechanism of bicarbonate reaction with hydrogen peroxide (eq 1) consists of the formation of carbon dioxide as an intermediate and reaction of CO_2 with hydrogen peroxide (as H_2O_2 and HOO^-), as shown in Scheme 1. We note that the rate constants and pH dependence indicate that both pathways contribute significantly to the addition of peroxide to carbon dioxide, even at neutral pH. The rate of CO_2 disappearance is determined by hydration, perhydration, hydroxide, and hydroperoxide addition reactions (reactions M3, M4, M5, and M8, Table 1) and is given by eq 10. The rate constants k_{-3} and k_{-4} represent the well-known pathways of hydration and hydroxide addition, respectively. Below pH 8 and in the absence of peroxide the hydration pathway predominates, while at the highest pH values in the present work (~8.5) the two pathways are comparable.

$$-\frac{d[CO_2]}{dt} = \{k_5[H_2O_2] + k_8[OOH^-] + k_{-3} + k_{-4}[OH^-]\}[CO_2] \quad (10)$$

The hydration pathway is subject to catalysis by simple oxyanions.[57] From the present work we cannot determine

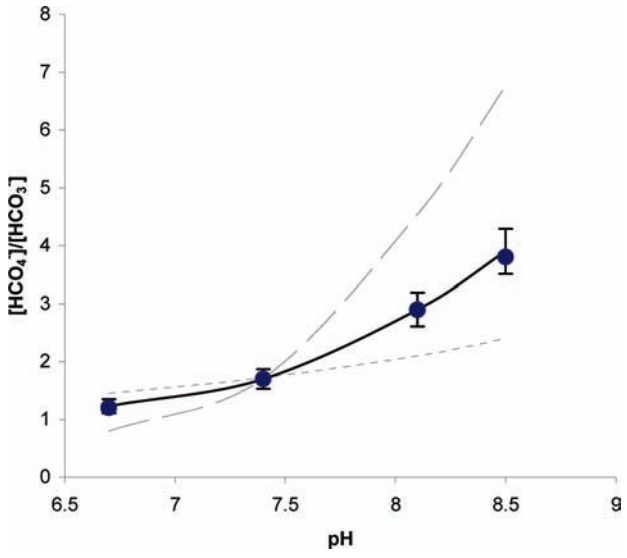

Figure 7. Initial ratio of $[HCO_4^-]/[HCO_3^-]$ ($t \approx 20$ s). (●) Experimental results from ^{13}C NMR spectra at various pH values; (solid line) simulation curve with $k_5 = 0.019\ M^{-1}\ s^{-1}$ and $k_8 = 280\ M^{-1}\ s^{-1}$, see Table 1; (dashed line) simulation curve with $k_5 = 0.0082\ M^{-1}\ s^{-1}$ and $k_8 = 560\ M^{-1}\ s^{-1}$; (dotted line) simulation curve with $k_5 = 0.025\ M^{-1}\ s^{-1}$ and $k_8 = 140\ M^{-1}\ s^{-1}$. The latter two curves demonstrate the sensitivity of the predicted ratios as a function of pH to the values of k_5 and k_8 used in the simulations. Error limits show the estimated 10% error in the ratios determined by NMR integrations.

whether anions also contribute to the rate of perhydration, so the estimated rate constants for reactions M5 and M8 will also contain any contributions from acetate and/or phosphate catalysis. Above pH ~8, the OOH^- pathway will contribute more to perhydration than percarbonic acid formation by direct addition of H_2O_2.

On the basis of our rate constants HOO^- is a stronger nucleophile than H_2O_2 toward the carbon center in CO_2 by a factor of $\sim 10^4$. For comparison, higher relative reactivities for OOH^- are also observed in the nucleophilic oxidation of dimethylsulfoxide (DMSO) and dimethyl sulfide (DMS) by hydrogen peroxide, where $k(HOO^-)$ was ~30 and 100 times higher than $k(H_2O_2)$.[59] H_2O_2 reacts with carbon dioxide more rapidly than water (the second order rate constant for water as a nucleophile, estimated from k_{-3} and adjusting for the concentration of water, is $\sim 8 \times 10^{-5}\ M^{-1}\ s^{-1}$, compared to $0.02\ M^{-1}\ s^{-1}$ for H_2O_2). As a result, 1 M hydrogen peroxide is competitive with H_2O for the reactive intermediate CO_2 even though it is at a much lower effective concentration than water itself (i.e., $k_5[H_2O_2] + k_8[HOO^-] \approx k_{-3}$). The estimated rate constant ($k_8 = 280\ M^{-1}\ s^{-1}$) for the reaction of HOO^- with CO_2 is substantially lower than that for OH^- ($k_{-4} = 8500\ M^{-1}\ s^{-1}$); therefore, the α-nucleophile effect is not strongly operative in base-catalyzed perhydration, as also concluded by Dennard and Williams.[57]

Anbar and Taube have studied the reaction of nitrite (NO_2^-) with hydrogen peroxide.[60] The formation of the proposed intermediate (NO^+) is analogous to CO_2 formation in the HCO_3^- reaction with H_2O_2 (i.e., the reactive intermediate is the anhydride of the protonated parent acid, $H_2NO_2^+$). We used the ratio of rate constants for perhydration and hydration of NO^+ (2.4) and the known CO_2 hydration rate constant (reaction M3, Table 1) to estimate the expected rate constant for perhydration of CO_2 (k_5). The predicted value is $\sim 1 \times 10^{-2}\ M^{-1}\ s^{-1}$ and is consistent with the value of k_5 obtained in the present work ($0.02\ M^{-1}\ s^{-1}$).

Hurst et al. studied the reaction of CO_2 with peroxynitrite $ONOO^-$, and the rate constant ($2.9 \times 10^4\ M^{-1}\ s^{-1}$) is ~100-fold greater than that of HOO^- reaction with CO_2.[61] The peroxynitrite adduct rapidly decomposes and in part forms the homolytic cleavage products $NO_2\bullet$ and $CO_3^{\bullet -}$. We have not observed evidence for spontaneous homolytic cleavage in the chemistry of peroxymonocarbonate.

CO_2 as an Intermediate in Peroxymonocarbonate Formation. A key feature of the bicarbonate reaction with hydrogen peroxide is that the equilibrium formation of the reactive anhydride (CO_2) is strongly favored ($HCO_3^- + H^+ = CO_2 + H_2O$, $K' = K_2K_3 = 1.9 \times 10^6\ M^{-1}$) relative to many other common organic and inorganic acids in solution near a neutral pH value. The large value of K' is key to the facile HCO_3^- conversion to peroxymonocarbonate at neutral pH. The rate law for the initial formation of HCO_4^- upon mixing equilibrated HCO_3^- and H_2O_2 near neutral pH can be written as in eq 11 (the HOO^- contribution is relatively low at pH = 7).

$$\frac{d[HCO_4^-]}{dt} = K'[H^+][HCO_3^-](k_5[H_2O_2] + k_8[HOO^-]) \quad (11)$$

In comparisons to other acids (HNO_2, HSO_4^-, etc.), it is noted that similar equilibrium reactions to form reactive anhydride intermediates are not so strongly favored at neutral pH. For example, based on the study by Bayliss et al.,[62] $K' = 3.0 \times 10^{-7}\ M^{-1}$ for the equilibrium $H^+ + HNO_2 = NO^+ + H_2O$. The rate law for reaction $HNO_2 + H_2O_2 \rightarrow HNO_3 + H_2O$ was reported to be $-d[H_2O_2]/dt = k[H^+][HNO_2][H_2O_2]$ with $k = 134\ M^{-2}\ s^{-1}$ (presumably HOONO is the intermediate product and $-d[H_2O_2]/dt = d[HOONO]/dt$). Although NO^+ is more reactive toward H_2O_2 than CO_2, the overall value of $k = 134\ M^{-2}\ s^{-1}$ is ~200 times lower than the value of k_5K' ($2.6 \times 10^4\ M^{-2}\ s^{-1}$) in eq 11 for the reaction $HCO_3^- + H_2O_2 \rightarrow HCO_4^- + H_2O$. Therefore, practical peroxyacid formation can only be achieved at low pH values for HNO_2 and most common acids other than HCO_3^-. It is noteworthy, however, that the peroxide adducts of borates are also formed readily in mildly alkaline solutions and are reported to be effective oxidants in the borate catalysis of peroxide oxidations.[34]

Catalysis by Carbonic Anhydrase and a Zinc Model Complex. We have studied the equilibration kinetics for eq 1 by ^{13}C NMR in the presence of 10 μM carbonic anhydrase at pH = 7.4. The equilibration of peroxymonocarbonate with bicarbonate ion was complete in the time required to obtain the initial NMR spectrum ($t_{1/2} < 60$ s versus $t_{1/2}$ ~300 s in the absence of catalyst at 2 M H_2O_2). On the basis of the proposed mechanism (Scheme 1), the rate of equilibration of HCO_3^- with H_2O_2 (eq 1) can be accelerated if

(59) Amels, P.; Elias, H.; Wannowius, K. J. *J. Chem. Soc., Faraday Trans.* **1997**, *93*, 2537–2544.
(60) (a) Anbar, M.; Taube, H. *J. Am. Chem. Soc.* **1954**, *79*, 6243–6247. (b) Benton, D. J.; Moore, P. *J. Chem. Soc.* **1970**, 3179–3182.
(61) Lymar, S. V.; Hurst, J. K. *J. Am. Chem. Soc.* **1995**, *117*, 8867–8868.
(62) Bayliss, N. S.; Watts, D. W.; Dingle, R.; Wilkie, R. J. *Aust. J. Chem.* **1963**, *16*, 933–942.
(63) Halfpenny, E.; Robinson, P. L. *J. Chem. Soc.* **1952**, 928–938.

the CO_2 hydration equilibrium is catalyzed by carbonic anhydrase or other hydration/dehydration catalysts. We also investigated a zinc model compound for the active site of carbonic anhydrase, 1,4,7,10-tetraazacyclododecanezinc(II).[49] ^{13}C NMR studies show that the equilibration rate of HCO_3^- with 2 M hydrogen peroxide increases with increasing Zn(II) complex concentrations (0.001 M−0.01M) at pH 7.4. A low temperature study (10 °C) found a linear relationship between the observed rate constant of eq 1 and the concentration of $Zn(II)L^{2+}$ (data not shown). A $t_{1/2}$ value < 1 min is estimated from the initial NMR spectrum when $[Zn(II)L^{2+}] \geq 0.005$ M. With $[Zn(II)L^{2+}] = 0.001$ M, the initial spectrum indicates $t_{1/2} < 3$ min and the reaction is at equilibrium in ~10 min.

The experimental results for the zinc(II) model complex can be fit by kinetic simulations that include the known kinetic parameters for catalytic HCO_3^- dehydration and CO_2 hydration (reaction M9, Table 1). The catalysts for these reactions are reported to be $Zn(II)L(H_2O)^{2+}$ and $Zn(II)L(OH)^+$, respectively.[49] The reported catalytic rate constants k^d_{cat} and k^h_{cat} are listed in Table 1. With $[Zn(II)L^{2+}] = 0.001$M, $[Zn(II)L(H_2O)^{2+}]$ and $[Zn(II)L(OH)^+]$ are calculated to be 7.6×10^{-4} and 2.4×10^{-4} M, correspondingly at pH 7.4, based on a pK_a value of 7.9 for $Zn(II)L(H_2O)^{2+}$.[49] Kinetic simulations with conditions $[HCO_3^-]_0 = 0.1$ M and $[H_2O_2]_0 = 2$ M at pH 7.4 in the presence of 0.001 M $Zn(II)L^{2+}$ were used to produce concentration versus time profiles for eq 1. The simulations show that the $t_{1/2}$ for HCO_4^- formation is ~2 min, and, in agreement with the experimental results, the reaction takes approximately 10 min to complete five half-lives. The equilibrium reaction under the same conditions in the absence of zinc(II) complex has $t_{1/2} \approx 5$ min. It is not necessary to include the reaction of a Zn-OOH species in the simulation to model the experiment, although the reaction of a zinc-hydroperoxide complex with CO_2 is reasonable by analogy with reaction M9 in Table 1.

(64) Chance, B.; Greenstein, D. S.; Roughton, F. J. W. *Arch. Biochem. Biophys.* **1952**, *37*, 301–321.

Although carbonic anhydrase and a functional model complex accelerate HCO_4^- formation under our experimental conditions, the biological relevance of the chemistry is certainly not established since competing reactions need to be considered. For example, formation of HCO_4^- from hydrogen peroxide in the presence of bicarbonate/CO_2 buffer (eq 11) competes with the catalase enhanced decomposition of peroxide[64] and its other reactions, and even at low concentrations of catalase (~10^{-6} M) the formation of HCO_4^- would be insignificant.

Conclusions

Kinetic simulations of double pH jump experiments have established that the mechanism of bicarbonate (HCO_3^-) reaction with hydrogen peroxide involves the formation of CO_2 as an intermediate and the subsequent reaction of CO_2 with H_2O_2 and its conjugate base HOO^-. The rate constants for CO_2 reactions with H_2O_2 and HOO^- to form peroxymonocarbonate (HCO_4^-) have been estimated. The contribution of HOO^- to initial HCO_4^- formation increases with increasing pH, dominating above pH 8.

Formation of preoxymonocarbonate by the reaction of HCO_3^- with H_2O_2 can be significantly accelerated by carbonic anhydrase and a zinc(II) model complex for the enzyme. The chemistry of the CO_2/HCO_3^- equilibrium allows for the crucial biological transport and release of the carbon waste product of aerobic metabolism. It is now clear that the same equilibrium also allows for facile formation of peroxymonocarbonate ion at physiological pH values by reaction of CO_2 with hydrogen peroxide and its conjugate base. The possible biological significance of peroxymonocarbonate must be considered in light of its relatively slow formation rate from bicarbonate via the CO_2 pathway described here.

Acknowledgment. This work was supported by grants from the Army Research Office and ECBC (ARO 37580-CH-2). The authors thank Jessica Leigh for performing ^{13}C NMR experiments on the transfer of CO_2 gas in the tube headspace into buffered analyte solutions.